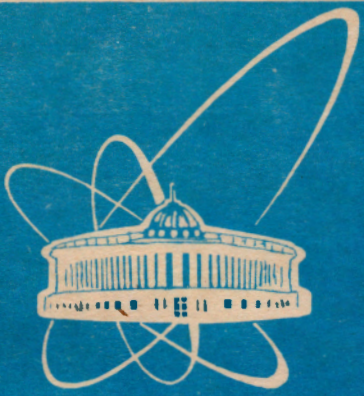

объединенный
институт
ядерных
исследований
дубна

E4-94-510

V.O.Nesterenko[1], W.Kleinig[2], V.V.Gudkov[3]

COLLECTIVE $E\lambda$-EXCITATIONS OF SURFACE CHARACTER IN SPHERICAL AND DEFORMED SODIUM CLUSTERS: VIBRATING POTENTIAL MODEL

Submitted to «Zeitschrift für Physik D»

[1]E-mail: nester@thsun1.jinr.dubna.su
[2]On leave of absence from Technical University Dresden, Institute for Analysis, Dresden, Germany
E-mail: kleinig@thsun1.jinr.dubna.su
[3]Department of Nuclear Physics, Charles University, V Holesovickach 2, CS-18000 Praha 8, Chekhia

1994

1 Introduction

Collective excitations (CE) associated with surface plasma oscillations are now a field of extensive investigation in alkali metal clusters (see, for example, recent papers [1-22] and refs. therein). Experimental data clearly demonstrate a resonance structure of these oscillations [1-7]. Most of the experimental and theoretical investigations are devoted to the electric dipole (E1) resonance. Information about electric resonances of higher multipolarity is very scarce and limited mainly by theoretical estimations [15,19,21,23].

Valence electrons in alkali clusters are often considered as moving in the mean field with shells like in atomic nuclei [24,25]. Single-particle potential describing this mean field can be obtained in the self-consistent way [26,27] or approximated by some phenomenological potential [28-32]. Vibration of the mean field, which is described in terms of residual correlations, leads to appearance of collective $E\lambda$ excitations. It is known that investigation of CE is rather complicated in clusters with open shells, which possess quadrupole (as well as hexadecapole and octupole) deformation [5-7,28,30-35]. In these clusters deformation splitting and Landau damping can lead to a quite complicated picture of CE when collective strength is distributed over many peaks. On the other hand, investigation of CE in deformed clusters is very important: just a deformation splitting of the E1 resonance now provides the most reliable information about the magnitude of cluster's deformation. To overcome these troubles, the random phase approximation (RPA) with residual forces of the separable form is suitable. This approach provides the microscopic accuracy of numerical results without time consuming calculations. The self-consistent version of this approach, so called vibrating potential model (VPM)[15,36,37], is especially attractive. In the VPM the form of residual forces and their strength constants are consistent with the form of the single-particle potential including all its deformation distortions. Moreover, the self-consistency condition between variations of the single-

particle potential and the corresponding ground state density provides the analytical expression for the strength constants. As a result, the model has no any adjusting parameters.

The VPM was firstly suggested in nuclear physics [36-40]. In [15] the main equations of the VPM for metal clusters were derived. If the Coulomb terms are neglected the equations [15] turn out to be suitable for the description of isoscalar giant resonances in atomic nuclei. So, the model is convenient for the comparison of collective excitations in clusters and atomic nuclei. Up to now, numerical calculations within the VPM in both atomic nuclei and metal clusters were limited to the case of the harmonic oscillator potential with quadrupole deformation (see, for example, [38,41]). In this paper, a more general version of the model (a generalized VPM (GVPM) [42-44]) is described. Using the multipole expansion of the single-particle potential and ground state density, we will obtain equations of the GVPM for systems with practically any kind of static deformation. Any single-particle potentials and ground state densities (including the ones calculated in the framework of the Kohn-Sham procedure), for which the coefficients of the multipole expansion are known, can be used within the model. Spherical systems are also covered.

Two features of the GVPM simplify the calculations. The first one is the separable form of the residual interaction. It should be noted that we use the total (without any truncation) multipole expansion of the Coulomb potential, i.e. we completely take into account a long-range character of the Coulomb forces. The second feature is the use of the strength function method [42,45]. This method allows one to avoid a direct solving of the RPA equations and to get information about CE through the strength function. As a result, the calculations are drastically simplified, which is very important for study of CE in large and deformed clusters.

In the present paper, the GVPM is described in detail (Sec.2). The

results of calculations within the GVPM for surface E1, E2 and E3 resonances in spherical (Na_8, Na_{20}, Na_{40}) and deformed (Na_{10}, Na_{18}, Na_{26}) sodium clusters are presented. For deformed clusters, axial quadrupole and hexadecapole deformations are taken into account. Both prolate (Na_{10}, Na_{26}) and oblate (Na_{18}) shapes are considered. Triaxial quadrupole deformation in these clusters is known to be negligible [5,10,35]. A mean field is approximated by the Woods-Saxon potential. Preliminary simplified results of the GVPM calculations for the E1 resonance in spherical sodium clusters were published in [44]. The results of present calculations are discussed in Sec.3. Conclusions are given in Sec.4.

2 Generalized vibrating potential model

2.1 Main equations of the VPM

In this subsection main equations of the VPM [15] are briefly reminded. We start with the energy functional for a system of N_e valence electrons in the external field of ions

$$E\{n(\vec{r},t),\tau(\vec{r},n(\vec{r},t))\} = 1/2\int \tau(\vec{r},t)d\vec{r} + \int v(\vec{r},t)d\vec{r} + 1/2\int\int \frac{(n(\vec{r},t)-n_i(\vec{r}))(n(\vec{r}_1,t)-n_i(\vec{r}_1))}{|\vec{r}-\vec{r}_1|}d\vec{r}d\vec{r}_1 \quad (1)$$

where

$$n(\vec{r},t) = \sum\nolimits_k |\phi_k(\vec{r},t)|^2 \quad (2)$$

and

$$\tau(\vec{r},t) = \sum\nolimits_k |\bigtriangledown \phi_k(\vec{r},t)|^2 \quad (3)$$

are the ground state density and kinetic energy density of valence electrons, respectively. Further, $n_i(\vec{r})$ is the ionic density in the jellium approximation, $\phi_k(\vec{r},t)$ is a single-particle wave function. Summation in (2) and (3) is performed over all occupied single-particle levels. The functional (1) includes the kinetic, exchange-correlation and Coulomb terms,

respectively. The latter embraces electron-electron (e-e), electron-ion (e-i) and ion-ion (i-i) interactions. In this section we will keep the convention $e = m_e = \hbar = 1$ where e and m_e are charge and mass of an electron.

The time dependent single-particle potential is obtained as

$$H(\vec{r},t)\phi_k(\vec{r},t) = \frac{\delta E}{\delta \phi_k^*(\vec{r},t)} = (-\frac{\nabla^2}{2} + V(\vec{r},t))\phi_k(\vec{r},t) \quad (4)$$

where

$$V(\vec{r},t) = \frac{dv}{dn} + \int\int \frac{(n(\vec{r}_1) - n_i(\vec{r}_1))}{|\vec{r} - \vec{r}_1|} d\vec{r}_1. \quad (5)$$

If the collective motion results in the density changing $\delta n(\vec{r},t)$, the Hamiltomian (4) can be divided into the static part

$$H_0(\vec{r}) = -\frac{\nabla^2}{2} + (\frac{dv}{dn})_{n=n_0} + \int \frac{n_0(\vec{r}_1) - n_i(\vec{r}_1)}{|\vec{r} - \vec{r}_1|} d\vec{r}_1 \quad (6)$$

and the time-dependent dynamical part

$$\delta H(\vec{r},t) = (\frac{d^2v}{dn^2})_{n=n_0} \delta n(\vec{r}_1,t) + \int \frac{\delta n(\vec{r}_1,t)}{|\vec{r} - \vec{r}_1|} d\vec{r}_1 \quad (7)$$

where $n(\vec{r},t) = n_0(\vec{r}) + \delta n(\vec{r},t)$ and $n_0(\vec{r})$ is the static ground state density. It is seen from (7) that variations of the density and single-particle potential are consistent.

It is convenient to express the density variation through the displacement field $\vec{u}(\vec{r})$ as $\delta n(\vec{r},t) = \alpha(t)((\nabla \cdot \vec{u})n_0 + \vec{u} \cdot \nabla n_0)$ where $\alpha(t)$ is an amplitude of the collective motion [15,46]. In the present paper, the simplest case of the irrotational and divergency free collective mode ($\nabla \times \vec{\omega} = \nabla \vec{u} = 0$ where $\vec{\omega}(\vec{r},t) = -\dot{\alpha}(t)\vec{u}(\vec{r})$) is considered. The displacement field is chosen as $\vec{u}(\vec{r}) = \nabla f(\vec{r})$ with $f(\vec{r}) = r^\lambda Y^d_{\lambda\mu}(\Omega)$ and $Y^d_{\lambda\mu}(\Omega) = Y_{\lambda\mu}(\Omega) + d \cdot Y^\dagger_{\lambda\mu}(\Omega)$. Here, $Y_{\lambda\mu}(\Omega)$ is the spherical harmonic, the coefficient $d = \pm 1$ assures the hermiticity of the Hamiltonian. Then, the density variation has the form $\delta n(\vec{r},t) = \alpha(t)(\nabla f(\vec{r}) \cdot \nabla n_0(\vec{r}))$ (for the sake of simplicity, in this subsection we will omit indices $\lambda\mu$ and d). This kind of collective motion is proportional to $\nabla n_0(\vec{r})$, i.e. is of the surface character.

Due to a considerable electrostatic screening between electron and ion fields (this is the exact case if the electron density is taken in the jellium approximation $n_0 = n_i$) the contribution of a direct Coulomb interaction to the static single-particle Hamiltonian (6) can be neglected [47] and we can use for the static single-particle potential the ansatz $V_0(\vec{r}) = (\frac{dv}{dn})_{n=n_0}$. Then, substituting the expression for $\delta n(\vec{r},t)$ into (7), one gets

$$\delta H(\vec{r},t) = \alpha(t) Q(\vec{r}) \quad (8)$$

where

$$Q(\vec{r}) = \nabla V_0(\vec{r}) \cdot \nabla f(\vec{r}) + \int \frac{\nabla n_0(\vec{r}_1) \cdot \nabla f(\vec{r}_1)}{|\vec{r} - \vec{r}_1|} d\vec{r}_1. \quad (9)$$

Following the condition of consistency between dynamical variations of the single-particle potential and density, one can rewrite (8) as

$$\delta H(\vec{r},t) = -\kappa \bar{Q}(t) Q(\vec{r}) \quad (10)$$

where $\bar{Q}(t) = \int Q(\vec{r}) \delta n(\vec{r},t) d\vec{r}$ and

$$\kappa^{-1} = \int n_0(\vec{r}) \nabla Q(\vec{r}) \cdot \nabla f(\vec{r}) d\vec{r} = -\int Q(\vec{r}) \nabla f(\vec{r}) \cdot \nabla n_0(\vec{r}) d\vec{r} \quad (11)$$

has the meaning of the inverse strength constant of the residual interaction (9). Substituting the Hamiltonian $H(\vec{r},t) = H_0(\vec{r}) + \delta H(\vec{r},t)$ to the time dependent Schrödinger equation, one finally gets the dispersion equation

$$X_t \equiv 2 \sum_{kk'} \frac{< k'|Q|k >^2 \epsilon_{kk'}}{\epsilon^2_{kk'} - \omega_t^2} = \kappa^{-1} \quad (12)$$

where $\epsilon_{kk'} = \epsilon_k + \epsilon_{k'}$ is the energy of a particle-hole excitation, $| k >$ and ϵ_k are the single-particle eigenstate and eigenenergy of the static hamiltonian (6), ω_t is the root of eq. (12).

Equations (9), (11) and (12), determining the form of residual forces, strength constant and dispersion equation, form the basis of the VPM [15]. If one neglects the Coulomb terms, these equations can be used to study isoscalar giant resonances in atomic nuclei.

2.2 Specification for deformed and spherical clusters

Equations (9),(11) and (12) are too general to be effectivelly used in practical calculations. One can get more concrete and convenient equations for deformed (and spherical) clusters [42-44] using the multipole expansion of the single-particle potential $V_0(\vec{r}) = \sum_l \sum_{m=-l}^{l} V_{lm}(r) Y_{lm}^d(\Omega)$ and ground state density $n_0(\vec{r}) = \sum_l \sum_{m=-l}^{l} n_{lm}(r) Y_{lm}^d(\Omega)$. Omitting tedious mathematical transformations we present the final expression for the operator (9):

$$Q_{\lambda\mu}^{(d)}(\vec{r}) = \sum_{LM} Y_{LM}(\Omega) \cdot \sum_{lm} (C_{lm\lambda\mu}^{LM} + d(-1)^{\mu} C_{lm\lambda-\mu}^{LM})(Q_{\lambda Llm}^{(v)}(r) + Q_{\lambda Llm}^{(c)}(r)) \tag{13}$$

where

$$Q_{\lambda Llm}^{(v)}(r) = (2\lambda+1)\sqrt{\frac{\lambda(2\lambda-1)}{\pi(2L+1)}} \cdot [M_{\lambda Ll}^{(1)} \frac{dV_{lm}}{dr} r^{\lambda-1} - M_{\lambda Ll}^{(2)} V_{lm} r^{\lambda-2}], \tag{14}$$

$$Q_{\lambda Llm}^{(c)}(r) = (2\lambda+1)\sqrt{\frac{\lambda(2\lambda-1)}{\pi(2L+1)}} \cdot (-\frac{4\pi}{2L+1})$$

$$\cdot [M_{\lambda Ll}^{(3)} r^{-(L+1)} \int_0^r n_{lm}(r_1) r_1^{\lambda+L} dr_1 + M_{\lambda Ll}^{(4)} r^L \int_r^{\infty} n_{lm}(r_1) r_1^{\lambda-L-1} dr_1]. \tag{15}$$

Here, $C_{lm\lambda\mu}^{LM}$ is the Clebsch-Gordan coefficient. Expressions for $M_{\lambda Ll}^{(i)}$ are given in the Appendix.

Expression (13) has a clear physical meaning. The coupling of the $\lambda\mu$ excitation with the spherical ($l = 0$) and deformed ($l = 2, 4, 6, ...$) parts of the single-particle potential (and density) leads to the appearance in the residual interaction of the family of modes with the moments $\mid \lambda - l \mid \leq L \leq \lambda + l$. The parity of these modes coinsides with the parity of λ. Expression (13) shows that due to the self-consistency, the residual interaction takes into account all the deformation distortions of the single-particle potential and density. The terms (14) and (15) represent the contributions of the Coulomb exchange and correlations and of the direct Coulomb interaction, respectively.

The corresponding expression for the inverse strength constant (11) is rather cumbersome. It is presented in the Appendix. It should be noted that in any case the best way to calculate the strength constant is the direct numerical integrating by exp. (11).

For clusters of spherical shape ($l = m = 0$, $L = \lambda$) expressions (9) and (11) are drastically simplified :

$$Q_{\lambda\mu}^{(d)}(\vec{r}) = \lambda[Y_{\lambda\mu}(\Omega) + d \cdot Y_{\lambda\mu}^{\dagger}(\Omega)] \cdot [\frac{dV_0}{dr} r^{\lambda-1} - \pi r^{-(\lambda+1)} \int_0^r n_0(r_1) r_1^{2\lambda} dr_1] \tag{16}$$

and

$$\kappa_{\lambda\mu d}^{-1} = -2\lambda^2 d(1 + \delta_{\mu,0}) \int_0^{\infty} [\frac{dn_0}{dr}\frac{dV_0}{dr} + 4\pi n_0^2(r)] r^{2\lambda} dr, \tag{17}$$

where $n_0(r) = n_{00}(r) 2Y_{00} = n_{00}(r)/\sqrt{\pi}$ (the same for $V_0(r)$).

If all collective strength is assumed to be concentrated in one state (one-pole approximation), we can get from eqs. (9), (11) and (12) the estimation

$$\omega_{\lambda\mu}^2 = (\omega_{\lambda\mu}^{(0)})^2 + \frac{\int (\nabla Q_{\lambda\mu}(\vec{r}))^2 \cdot n_0(\vec{r}) d\vec{r}}{\int Q_{\lambda\mu}(\vec{r}) \nabla f(\vec{r}) \cdot \nabla n_0(\vec{r}) d\vec{r}} \tag{18}$$

where $\omega_{\lambda\mu}$ and $\omega_{\lambda\mu}^{(0)}$ are the energy of the collective state and its unperturbed value, respectively. The expression for the square of the single-particle matrix element in (12) was obtained through the energy weighted sum rule for the operator (16). Using the step approximation $n_0(r) = n_0\Theta(r - R)$ for the density, the oscillator form $V_0(r) = 1/2 \cdot \omega_0^2 r^2$ for the single-particle potential and the estimation $\omega_{\lambda}^{(0)} = \lambda\omega_0$ for the unperturbed energy, we obtain the simple expression for excitation energy of the $E\lambda$ resonance in spherical clusters:

$$\omega_{\lambda} = \sqrt{\frac{\lambda}{2\lambda+1}\omega_p^2 + \omega_0^2\lambda(\lambda-1)} \tag{19}$$

where $\omega_p = \frac{4\pi n_0 e^2}{m}$ is the plasma frequency. Neglecting the first (Coulomb) term in (19) one gets the estimation for isoscalar giant resonances in

atomic nuclei: $\omega_\lambda = \omega_0\sqrt{\lambda(\lambda-1)}$. Expression (19) is in good agreement with the previous estimations obtained within the sum rule approach (SRA) [15,19] in spite of some difference in the λ dependence of the second term (in [19] the $\sim 2/5(2\lambda+1)(\lambda-1)$ dependence takes place).

2.3 Strength function method

For clusters with a large number of electrons a direct solving of the RPA equations can be very time consuming. This is especially true for deformed clusters where the number of states of a given multipolarity can be very large. On the other hand, for these systems we do not usually need a detailed information about all the states since, as a rule, experimental data provide only some averaged characteristics. For investigation of CE in these systems the strength function method is very useful. Using this method we can avoid finding roots of the secular equation (12) but get information about CE through the strength function [42,45]

$$b_m(E\lambda\mu,\omega) = \sum_t \omega_t^m B(E\lambda\mu, gr \rightarrow \omega_t)\rho(\omega-\omega_t) \qquad (20)$$

with the weight function

$$\rho(\omega-\omega_t) = \frac{1}{2\pi}\frac{\Delta}{(\omega-\omega_t)^2+(\Delta/2)^2}. \qquad (21)$$

Here, $B(E\lambda\mu, gr \rightarrow \omega_t)$ is the reduced probability of the $E\lambda\mu$ transition from the ground state to the one-phonon state with excitation energy ω_t. The quantity Δ is an averaging parameter. It is easy to see that for m=1 the strength function (20) has a form similar to the photo-absorption cross section for E1 resonance. Following ref. [45], where the strength function method was considered for atomic nuclei, one can get a quite general expression for the strength function of $E\lambda$ excitations in metal clusters [42]:

$$b_m(E\lambda,\omega) = \frac{1}{\pi}\left(Im\left(\frac{z^m\tilde{X}^2(z)}{X(z)-\kappa^{-1}_{\lambda\mu d}}\right)_{z=\omega+i\Delta/2}\right.$$

$$\left. +\Delta\sum_{k<k'}(p^{\lambda\mu}_{kk'})^2\epsilon^m_{kk'}\left(\frac{(-1)^{m+1}}{(\omega+\epsilon_{kk'})^2+(\Delta/2)^2}+\frac{1}{(\omega-\epsilon_{kk'})^2+(\Delta/2)^2}\right)\right) \qquad (22)$$

where

$$\tilde{X}(z) = 2\sum_{kk'}\frac{<k'|Q|k>p^{\lambda\mu}_{kk'}\epsilon_{kk'}}{\epsilon^2_{kk'}-z^2} \qquad (23)$$

and $p^{\lambda\mu}_{kk'}$ is the single-particle matrix element for the standard operator of the $E\lambda\mu$ transition. Expression (22) is valid for m=0,1,2 and 3. It is easy to see that we do not need any one-phonon excitation energies and wave functions for calculation of the strength function (22). We do not need also any iteration procedures. As a result, one can get averaged characteristics of $E\lambda$ excitations without time consuming calculations.

3 Results of calculations and discussion

3.1 Details of calculations

The calculations within the GVPM have been performed for neutral spherical (Na_8, Na_{20}, Na_{40}) and deformed (Na_{10}, Na_{18}, Na_{26}) clusters. The E1 resonance was considered for all these clusters. The E2 and E3 resonances were calculated for Na_{40} and Na_{26}.

A mean field was approximated by the Woods-Saxon potential

$$V_0(\vec{r}) = \frac{U_0}{1+exp[(r-R(\Omega))/a_0]} \qquad (24)$$

with $R(\Omega) = R_0(1+\beta_0+\beta_2Y_{20}(\Omega)+\beta_4Y_{40}(\Omega))$ and $R_0 = r_0N_e^{1/3}$. Here, β_2 and β_4 are the parameters of quadrupole and hexadecapole deformation, the parameter β_0 ensures the conservation of the cluster volume.

The Woods-Saxon potential is known to reproduce rather well the form of the single-particle field obtained in the self-consistent calculations for a wide group of sodium clusters [29]. This potential was successfully used for determining magic numbers [29] and equilibrium deformations [33,34] in sodium clusters. In our calculations, the depth and radius parameters of the potential (24) are taken from [29]: $U_0 = -6eV$, $r_0 = 2.25\AA$.

The value of diffuseness parameter, $a_0 = 0.74\mathring{A}$, used in [29] is not suitable for our calculations. As has been mentioned in [29], at this value of a_0 the potential (24) vanishes faster than in the self-consistent Kohn-Sham calculations [24], i.e., the diffuseness parameter in [29] is underestimated. Moreover, due to a local density approximation for the Coulomb exchange, the Kohn-Sham calculations are also known to underestimate the surface diffuseness (in terms of the "spill-out") [23]. In our calculations the diffuseness parameter a_0 has to be chosen more carefully since this parameter influences the energy positions of $E\lambda$ resonances of the surface character. After a comprehensive analysis the value $a_0 = 1\mathring{A}$ was chosen. At this value, our calculations reproduce rather well, for example, the percentage of the spilled out electrons (19%) in Na_8, obtained the Kohn-Sham calculations [47] (see Table 1). Diffuseness of the single-particle potential should not be confused with diffuseness of the density of valence electrons in the ground state (the latter is calculated by exp. (2) using the single-particle wave functions of the potential (24)). For Na_8, Na_{20} and Na_{40} this density as well as the single-particle potential (24) are presented in Fig. 1. It is seen that diffuseness of the densities is smaller than that of the corresponding potentials. For Na_{40}, the potential and density are depicted for three values of the diffuseness: $a_0 = 1.4, 1.0$ and $0.74\mathring{A}$. As is seen, the variation of diffuseness in this range does not change the density much.

For deformed clusters, axial quadrupole $\lambda\mu = 20$ and hexadecapole $\lambda\mu = 40$ deformations were taken into account. The triaxial quadrupole deformation, $\lambda\mu = 22$, in these clusters can be neglected [5,10,35]. Both prolate (Na_{10}, Na_{26}) and oblate (Na_{18}) spheroidal shapes were considered. The parameters of deformation β_2 and β_4 are given in Table 1. For Na_{10}, these parameters were taken from the Kohn-Sham calculations [48] within the structure-averaged jellium model [12]. For Na_{18} and Na_{26}, the deformation parameters were estimated following ref. [10] (see Table 1 and Appendix in [10]). The multipole expansions for potential $V_0(\vec{r})$ and

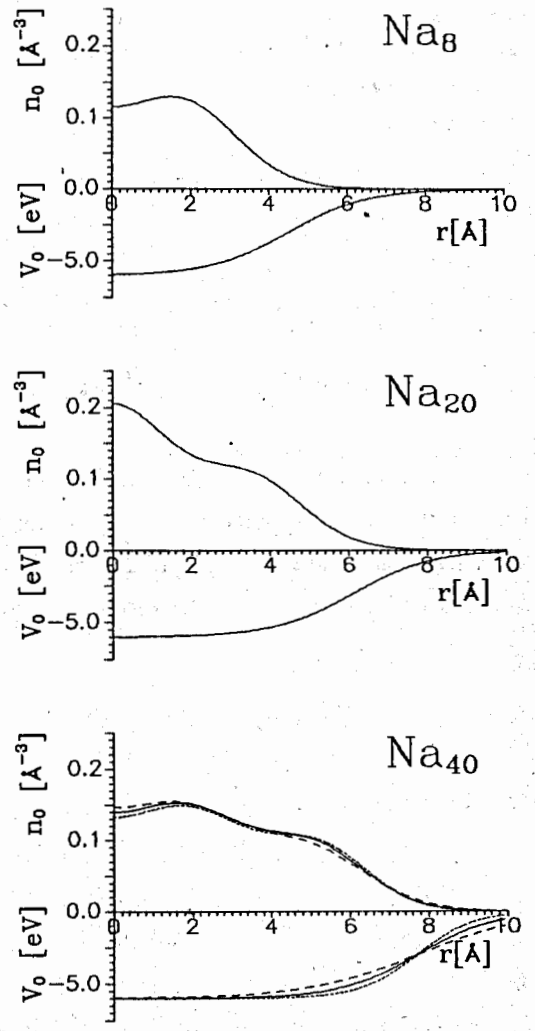

Fig. 1. The density of valence electrons (2) and the Woods-Saxon single-particle potential (24) for Na_8, Na_{20} and Na_{40}. For Na_{40} the results are given for diffuseness $\alpha = 1.4$ (dashed line), 1.0 (solid line) and 0.74 $\mathring{A}$ (dotted line).

Table 1: Deformation parameters β_2 and β_4, amount of the spilled out electrons δN and model-independent energy weighted sum rules $S(\lambda=1)$ for clusters under consideration. Following [47], δN was calculated as an amount of electrons (in %) outside the sharp jellium border at $R = r_0 N^{1/3}$ with $r_0 = 2a.u. = 2.116\mathring{A}$.

Cluster	Na_8	Na_{20}	Na_{40}	Na_{10}	Na_{18}	Na_{26}
β_2	0	0	0	0.384	0.23	0.40
β_4	0	0	0	0.212	0.02	0.06
$\delta N, \%$	20	13	10	20	14	12
$S(\lambda=1), e^2eV\mathring{A}^2$	21.8	54.5	109	27.3	49.1	70.9

density $n_0(\vec{r})$ were limited by the terms with $l = 0, 2, 4$ and 6. The calculations show that the influence of the terms with $l > 6$ can be neglected.

The completeness of the single-particle basis for the description of $E\lambda$ excitations is usually estimated to be sufficient if the model-independent energy-weighted sum rule

$$S(\lambda) = \sum_i \omega_i B(E\lambda, gr \rightarrow \omega_i) = \frac{\hbar^2 e^2}{8\pi m_e}\lambda(2\lambda+1)^2 N < r^{2\lambda-2} > \qquad (25)$$

is exhausted to a large extent. The radial part $r^{2\lambda-2}$ is averaged over the ground state. The values $S(\lambda=1) = \frac{\hbar^2 e^2}{8\pi m_e} 9N$ for clusters under consideration are presented in Table 1. In our calculations E1 excitations, in the energy interval 1-6 eV exhaust practically 100% of the sum rule (25). E2 and E3 excitations in the same energy interval exhaust $90-100\%$. So, the single-particle basis used in the present calculations is quite complete.

For E1 excitations the strength function $\sigma(E1,\omega) = b_{m=1}(E\lambda,\omega)$ was calculated. This strength function has the same energy multiplier as the photoabsorption cross section which is mainly used for experimental investigation of the E1 resonance. So, the strength function $\sigma(E1,\omega)$ is convenient for comparison with experimental data. This is not the case for the E2 and E3 resonances, for the experimental study of which

the inelastic electron scattering (e,e') seems to be more suitable. For E2 and E3 resonances we calculated the strength function with $m = 0$. The averaging parameter Δ was chosen to be equal to 0.05 eV, which corresponds to a thermal energy with $T \sim 500K$. The value $\Delta = 0.05eV$ is much smaller than the typical width of the E1 resonance (the latter is estimated as $10-15\%$ of the excitation energy). But so small averaging allows one to demonstrate the complicated structure of the resonances which often includes more than one collective peak.

3.2 Main results and discussion

Main results of the calculations are presented in Figs. 2-9 and Tables 2 and 3.

In Fig.2, the radial dependence of the operator (13) (or, in other words, of the residual forces) is demonstrated. The $\lambda\mu = 10$ excitation in the deformed Na_{26} is considered as an example. The parts of the operator (13), corresponding to the coupling of the dipole mode with spherical ($l = 0$) and quadrupole ($l = 2$) terms of the single-particle potential and density are depicted. Following the rule $|\lambda - l| \leq L \leq \lambda + l$, the coupling with the terms corresponding to the quadrupole deformation leads to appearance in (13) of parts with moments $L = 2$ and 4. For every part of the operator (13) the functions $Q^{(i)}_{\lambda Ll}(r) = (C^{L\mu}_{l0\lambda\mu} + d(-1)^{\mu} C^{L-\mu}_{l0\lambda-\mu}) Q^{(i)}_{\lambda Ll0}(r)$ representing contributions of the exchange-correlation (i=v) and direct Coulomb (i=c) terms, as well as their sum (i=v+c), are presented. It is seen that, in spite of rather large deformation of Na_{26}, the residual interaction is mainly determined by the spherical part of the single-particle potential and density (see the top of Fig.2). The contribution of the exchange-correlation term is much smaller and of the opposite sign as compared with the contribution of the direct Coulomb term. The calculations show also that in all the clusters just the direct Coulomb term mainly determines the residual interaction. Deformation corrections presented in the middle and bottom parts of Fig.2 are in total $10-15\%$

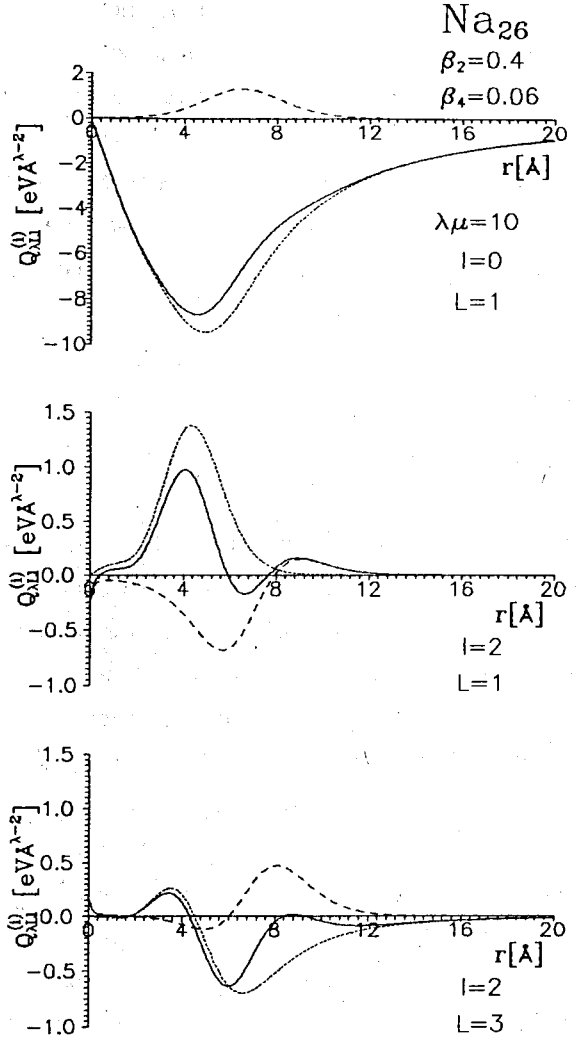

Fig.2 Radial dependence of the components $Q^{(i)}_{\lambda LI}(r)$ of the operator (13): the exchange-correlation part ($i = v$, dashed line), the Coulomb part ($i = c$, dotted line) and their sum ($i = v + c$, solid line). See comments in the text.

of magnitude of the main spherical part. It is seen that the exchange-correlation term exhibits relatively larger deformation corrections (up to 50%) than the Coulomb term. The deformation corrections caused by both these terms noticeably compensate each other. This means that in metal clusters the influence of deformation distortions should be relatively weaker than in atomic nuclei where only the term (14) takes place. Fig. 2 shows also that the residual interaction has a long Coulomb tail, i.e., takes into account a long-range character of the Coulomb forces.

The results of calculations for E1 excitations in the spherical Na_8, Na_{20} and Na_{40} are presented in Fig.3 and Table 2. The strength functions $\sigma(E1,\omega)$ are given in Fig.3 for two cases: with and without the residual interaction. In the latter case, we have $\kappa_{\lambda\mu d} = 0$ and E1 excitations are determined by pure particle-hole transitions of non-interacting electrons. Then, the E1 resonance lies in the region 1.0-1.5 eV that is much lower than the experimental value. The energy 1.0-1.5 eV is a typical energy interval between neighboring shells. In other words, this energy corresponds to E1 transitions with $\Delta N = 1$ where N is the principal shell quantum number. The self-consistent residual interaction shifts the resonance towards the energy 2.6-3.3 eV. For Na_8 and Na_{20} this energy is a little bit higher than the experimental values. In accordance with the experimental data [5,6], our calculations give one peak in Na_8 and two peaks in Na_{20}. As is seen from Fig.3, the calculations do not reproduce the tendency of approaching the classical Mie energy with increasing N_e. This tendency can be masked by shell effects but it is not the main reason in the present calculations. It is more important here that we use for all clusters one and the same averaged diffuseness parameter of the Woods-Saxon potential. As was mentioned above, this parameter influences much the position of the E1 resonance and, in principle, has to be adjusted for each cluster separately (for example, by calculation of the static dipole polarizability). This will be done in the subsequent papers. Also, the agreement with the experiment can be improved if we take into

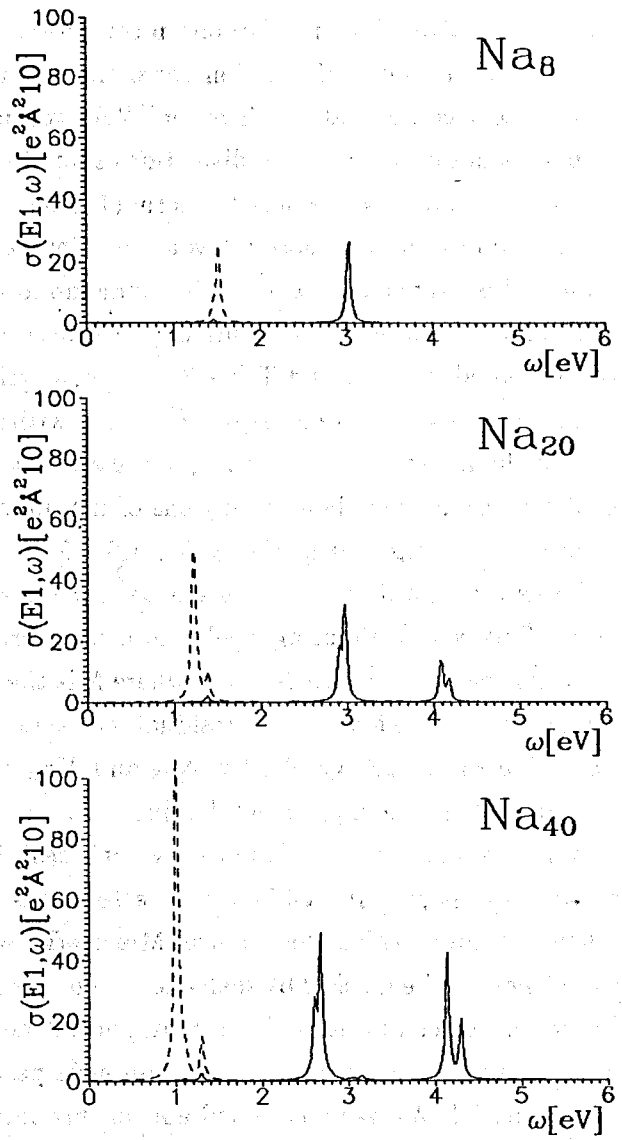

Fig.3 The strength function $\sigma(E1,\omega)$ for E1 excitations in Na_8, Na_{20} and Na_{40}.

Table 2: Experimental [5] and calculated within the GVPME and the SRA [10] excitation energies (ω, in eV) and deformation splittings ($\Delta\omega$, in eV) of the E1 resonance. For the GVPM the energy centroids of the resonance are given

Cluster	Na_8	Na_{20}	Na_{40}	Na_{10}	Na_{18}	Na_{26}
ω_{exp}	2.59	2.67	2.72	2.02,2.67	2.56,2.94	2.29,2.93
ω_{GVPM}	3.04	2.94	2.64	2.58,3.32	2.86,3.26	2.65,3.32
ω_{SRA}	2.77	2.94	3.05	2.28,3.03	2.79,3.18	2.50,3.24
$\Delta\omega_{exp}$	-	-	-	0.65	0.38	0.64
$\Delta\omega_{GVPM}$	-	-	-	0.74	0.40	0.67
$\Delta\omega_{SRA}$	-	-	-	0.75	0.39	0.74

account the volume (bulk) part of the residual interaction. This can be done by the replacement of the external field $f(\vec{r}) = r^\lambda Y^d_{\lambda\mu}(\Omega)$ by the field $f(q\vec{r}) = j_\lambda(qr)Y^d_{\lambda\mu}(\Omega)$ where q determines the proportions between bulk and surface excitations [43]. Following [23] the coupling of surface and volume excitations should lead to some decreasing the energy of the E1 resonance. In spite of some shortcomings of the present calculations, one should note that the agreement of our results with the experimental data for spherical clusters is quite satisfactory. In any case, this agreement is not worse than in the calculations within other models.

The results of calculations of E1 excitations in the deformed Na_{10}, Na_{18} and Na_{26} are exhibited in Figs.4-6. In Table 2 these results are compared with the available experimental data and the results obtained in the framework of the sum rule approach (SRA)[10]. As is seen from the figures, the deformation of clusters leads to a quite common picture. Namely, in Na_{10} and Na_{26}, that have a prolate quadrupole deformation, the small peak corresponding to vibrations of electrons along the z-axis of the spheroid has lower energy as compared with the large peak corresponding to vibrations of electrons along the x- and y-axes. In the cluster with oblate deformation, Na_{18}, the opposite picture takes place.

Due to the deformation splitting, resonances in Na_{18} and Na_{26} demonstrate the substantial Landau damping. Table 2 shows that for small deformed clusters the GVPM calculations also give somewhat overestimated energies of the E1 resonance. But note again that taking into account the the volume part of the residual interaction should improve the agreement with the experiment. The description of the deformation splitting is rather nice although this seems to be mainly a merit of the single-particle scheme. The comparison in Table 2 of the GVPM and SRA results indicate that these models provide more or less the same quality of description of excitation energies and deformation splittings of the E1 resonance. Nevertheless, the GVPM has an important advantage. This model can describe not only these two characteristics but also the Landau damping, i.e., fragmentation of the collective strength over many peaks. Our results for Na_{18} and Na_{26} show that the Landau damping is a quite general property of E1 excitations beginning from rather small clusters. Without doubt, this property should be taken into account for correct comparison with experimental data. (It is to be noted that fragmentation of the E1 resonance can be calculated also within other approaches: self-consistent model of W.Ekardt [14], full RPA [17,18] and local RPA [9-11,23]. But the calculations within these approaches are much more time consuming, especially for large and deformed clusters.)

It is interesting to estimate the collectivity of the states forming the E1 resonance. The large value of reduced transition probability $B(E1, gr \rightarrow \omega_i)$ does not always mean the strong collectivity of the state since this large value can be caused in some cases by a single (but strong) single-particle matrix element. To estimate the collectivity, the structure the state should be also considered. From a general point of view it is clear that the larger number of particle-hole configurations contribute to the state, the stronger its collectivity. In Table 3, the structure of the states in Na_{10}, Na_{18} and Na_{26} with maximal $B(E1)$ values is presented. It is seen that these states exhaust a large amount of the model-independent

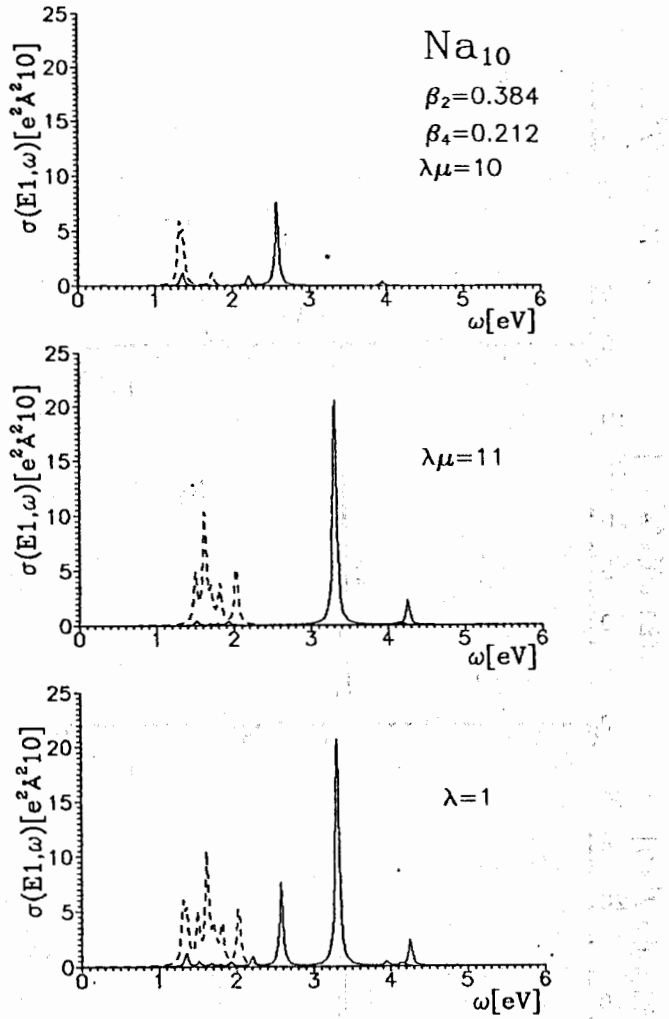

Fig.4 The strength function $\sigma(E1,\omega)$ for E1 excitations in Na_{10}. The plots are given for $\mu = 0$ (top), $\mu = 1$ (middle) and for total case (bottom). The results obtained with (solid line) and without (dashed line) the residual interaction are presented. See comments in the text.

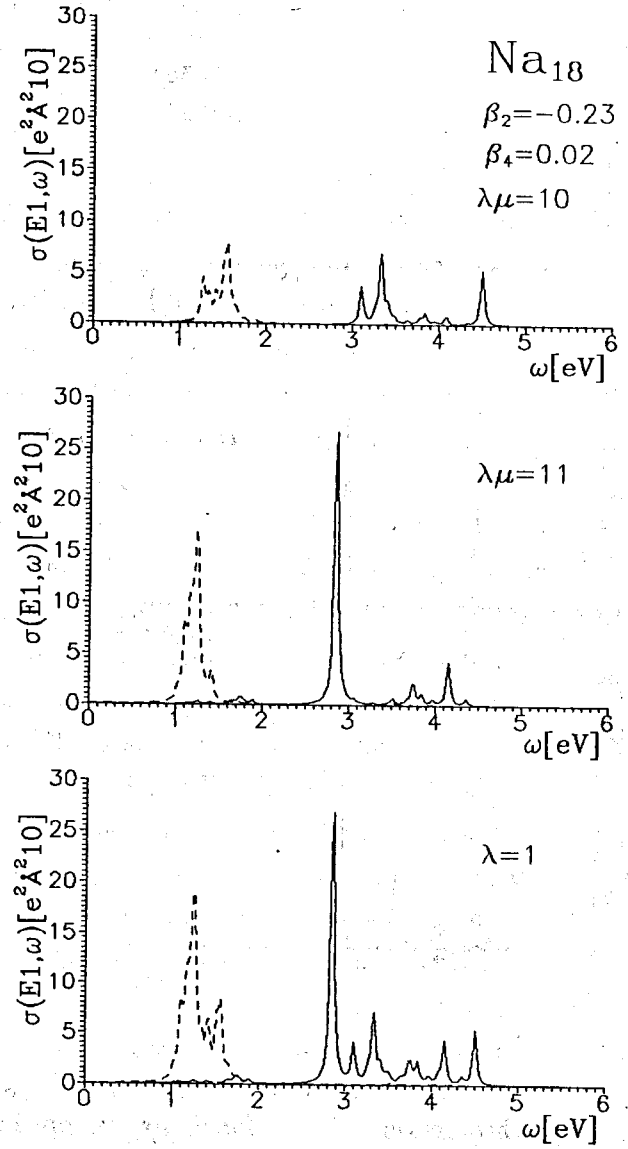

Fig.5 The same as in Fig.4 for Na_{18}.

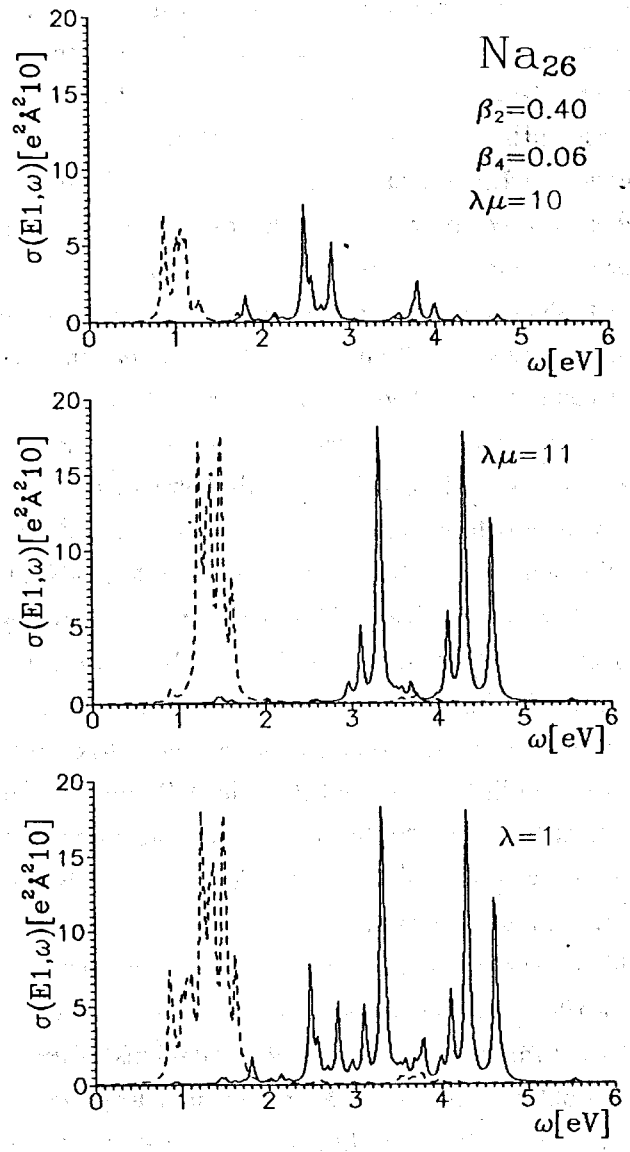

Fig.6 The same as in Fig.4 for Na_{26}.

sum rule $S(\lambda = 1)$. They are composed of a large number of particle-hole configurations corresponding to $\Delta N = 1$ and 3 dipole transitions. So, these states are really collective. Table 3 also shows that, on the average, the larger a cluster, the stronger collectivity of its states.

Figs.3-6 show that E1 excitations have pronounced high-energy peaks which are well separated from the main E1 resonance. These peaks take place in all clusters and the larger the cluster, the stronger the peaks. This tendency is demonstrated in Fig.3 for spherical clusters: while in Na_{10} high-energy peaks are absent at all, they appear in Na_{20} (the experimental data [5-7] suggest the two-peak structure of the E1 resonance in this cluster) and become very large in Na_{40}. As is seen from Figs.4-6 a similar situation takes place in deformed clusters as well. The high-energy peaks exhaust a large amount of the sum rule (25). In Na_{26} and Na_{40} the contribution of the peaks at the energy 4.0-4.8 eV into the sum rule is 28% and 44%, respectively. This is in some discrepancy with the experimental data [7] where for these clusters (but ionized) $80 - 100\%$ of the dipole sum rule was observed in the energy interval 2-3.4 eV. The coupling with the volume plasmon and the use of a larger averaging parameter Δ (corresponding to the realistic width $\Gamma = 0.15\omega$) should shift the dipole strength towards the lower energies and improve the agreement with the experiment. As our estimations show, in this case the high-energy peaks remain to be rather well separated from the main E1 resonance although they will have lower excitation energies.

The origin of the high-energy peaks is rather clear. They are nothing but the $\Delta N = 3$ branch of E1 collective excitations. Just due to the $\Delta N = 3$ nature of these peaks we have the tendency that the heavier cluster, the larger their strength. In Table 3, the structure of the high-energy state with $\omega = 4.31$ eV in Na_{26} is presented as an example. It is seen that the large components of this state are mainly formed by the particle-hole configurations with $\Delta N = 3$ while the small components determining the collectivity of the state — mainly by configurations with

$\Delta N = 1$. The residual interaction shifts the E1 $\Delta N = 1$ strength to the high-energy region of rather weak particle-hole excitations with $\Delta N = 3$ and promotes in this way the collective high-energy peaks. The long-range character of the Coulomb forces (furthering the interaction between electrons far from each other) also favours the formation of the $\Delta N = 3$ branch. This picture is of general character and concerns any $E\lambda$ excitations. As a result, the $E\lambda$ excitations seem to be attractive for investigation of the ΔN shell effects. In particular, the experimental observation of the $\Delta N = 3$ branch of the E1 resonance could be very interesting. This could confirm additionally the existence of shells in metal clusters.

As has been mentioned above, both experimental and theoretical studies of $E\lambda$ excitations with $\lambda > 1$ are at the initial stage. The $E\lambda(\lambda > 1)$ resonances were calculated within the SRA in [19] and within the fluid-dynamical approach (FDA) in [21]. In [15] the "scissors" quadrupole resonance in deformed clusters was analyzed within the SRA. Due to the inherent limitations of the SRA and FDM, these investigations do not take into account the fragmentation of the $E\lambda(\lambda > 1)$ resonances. On the other hand, the investigation of the $E\lambda(\lambda > 1)$ resonances in a similar Fermi system, atomic nuclei, clearly shows that the larger multipolarity of the resonance, the stronger its fragmentation. And just the large fragmentation is usually the main trouble in experimental search for these resonances. Also, due to the shell structure of cluster's mean field, the strength of the $E\lambda(\lambda > 1)$ excitations should be distributed between branches with $\Delta N = 1, ..., \lambda$ and $\Delta N = 0, ..., \lambda$ for odd- and even-parity excitations, respectively. It is clear that without taking into account these effects it is very difficult to make any realistic predictions for $E\lambda(\lambda > 1)$ resonances. This is just the advantage of the GVPM that this model can describe these effects.

One can estimate a lower limit for multipolarity of collective $E\lambda$ excitations: $\lambda \leq 0.7 r_0^{1/2} N_e^{1/3}$ [19]. For sodium clusters with $r_0 = 2.25\AA$ we

Table 3: Energies, $B(E1)$ values, contributions to the model-independent sum rule $S(\lambda = 1)$ and structure (contributions of main particle-hole configurations) of the states with maximal $B(E1)$ values in Na_{10}, Na_{18} and Na_{26}. Particle and hole excitations are classified following the convention of Clemenger [28] using Nilsson's asymptotic quantum numbers $Nn_z\Lambda$.

Cluster	Na_{10}	Na_{18}	Na_{26}
ω, eV	2.31	2.85	3.33
B(E1), $e^2\AA^2$	2.3	8.0	4.3
S(E1), %	20	44	19
	000,301 34%	202,303 27%	101,402 19%
	000,311 33%	211,312 21%	101,413 13%
	000,321 27%	101,422 9%	101,400 13%
	101,202 3%	220,330 5%	101,420 9%
Structure	110,211 2%	220,321 5%	202,303 8%
$(Nn_z\Lambda)_h(Nn_z\Lambda)_p$		110,431 5%	211,312 7%
		202,321 3%	200,301 5%
		211,321 2%	321,422 5%
ω, eV	3.31	3.33	4.31
B(E1), $e^2\AA^2$	5.5	1.6	3.6
S(E1), %	63	11	20
	101,202 41%	101,420 28%	110,411 29%
	110,211 30%	101,440 13%	101,402 22%
	101,200 8%	101,431 9%	000,301 18%
	000,321 7%	101,200 5%	202,303 6%
Structure	220,321 6%	202,301 5%	101,400 5%
$(Nn_z\Lambda)_h(Nn_z\Lambda)_p$	220,301 3%	211,310 4%	211,312 4%
	000,312 1%	202,303 4%	321,422 3%
	000,301 1%	101,422 4%	200,301 3%

have $\lambda \leq 1.05\AA N_e^{1/3}$. Following this estimation we can consider E2 and E3 collective excitations in clusters beginning with Na_{26}.

In Figs. 7-9 the strength functions $b(E\lambda,\omega) \equiv b_{m=0}(E\lambda,\omega)b_1(E\lambda,\omega)$ for E2 and E3 excitations in spherical Na_{40} and deformed Na_{26} are presented. For the first time, calculations of the E2 and E3 resonances were performed taking into account their fragmentation. As is seen from Fig.7, in the spherical Na_{40} the pure particle-hole E2 and E3 excitations demonstrate the particular shell behavior: these excitations are mainly formed by $E2(\Delta N = 2)$ transitions with energy about 2 eV and by $E3(\Delta N = 1,3)$ transitions with energies about 1 and 3 eV. The residual interaction shifts the strength of these transitions towards higher energies. As a result, the main E2 and E3 peaks are placed at 3.5 and 4.1 eV, respectively. These energies have to be considered as some maximal values since taking into account of the volume parts of E2 and E3 excitations should, in principle, decrease them. The most important point is.that the E2 and E3 resonances are not much fragmented so that they have a good chance to be measured in the (e,e') reaction. The E2 and E3 resonances in deformed Na_{26} are exhibited in Figs.8 and 9. These resonances are more fragmented than their counterparts in Na_{40} but, nevertheless, they remain to be well concentrated. So, the search for the E2 and E3 resonances in both spherical and deformed sodium clusters is quite realistic and is a challenge for experimentalists.

4 Conclusions

The generalized version of the vibrating potential model (GVPM) was proposed for the description of multipole $E\lambda$ excitations of the surface character in spherical and deformed alkali metal clusters. The model seems to be rather optimal in the sense that, on the one hand, it provides a microscopical quality of the description (energy position, fragmentation, etc.) and, on the other hand, does not need time consuming calcu-

lations. The latter is achieved by using the strength function method and the separable form of the residual interaction. The use of phenomenological single-particle potentials simplifies the calculations additionally. Being self-consintent, the model does not need any adjusting parameters and provides rather reasonable predictions. If the Coulomb terms are neglected the model can be used for the description of isoscalar giant resonances in atomic nuclei. So, the GVPM is convenient for comparison of $E\lambda$ excitations in atomic nuclei and metal clusters.

The results of calculations within the GVPM for E1, E2 and E3 resonances in spherical and deformed sodium clusters are presented. The results for the E1 resonance are in satisfactory agreement with the available experimental data. In particular, in deformed clusters both energy position and deformation splitting are described rather well. The calculations predict a group of high-energy peaks which form the $\Delta N = 3$ branch of E1 excitations and are rather well separated from the main E1 resonance.

Calculations for the E2 and E3 resonances, taking into account their fragmentation, have been performed for the first time. The calculations show that E2 and E3 resonances are well concentrated and have a good chance to be measured in the (e, e') reaction. The study of the E1, E2 and E3 resonances can provide valuable information about different properties of metal clusters. The deformation splitting of the E1 resonance can be used for confirmation and detailed investigation of cluster's deformation distortions. Also, E1, E2 and E3 resonances can be used to study ΔN splittings connecting with the shell structure of cluster's mean field.

In the subsequent papers, the volume $E\lambda$ excitations will be taken into account. The corresponding formalism is presented in ref.[43].

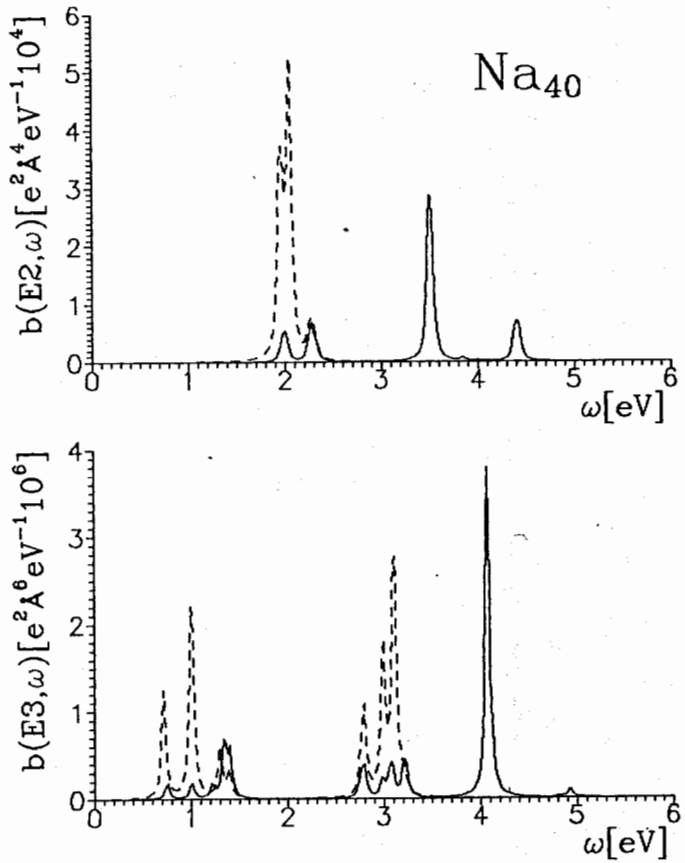

Fig.7 The strength function $b(E\lambda,\omega) \equiv b_{m=0}(E\lambda,\omega)$ for E2 and E3 excitations in Na_{40}. The results obtained with (solid line) and without (dashed line) the residual interaction are presented.

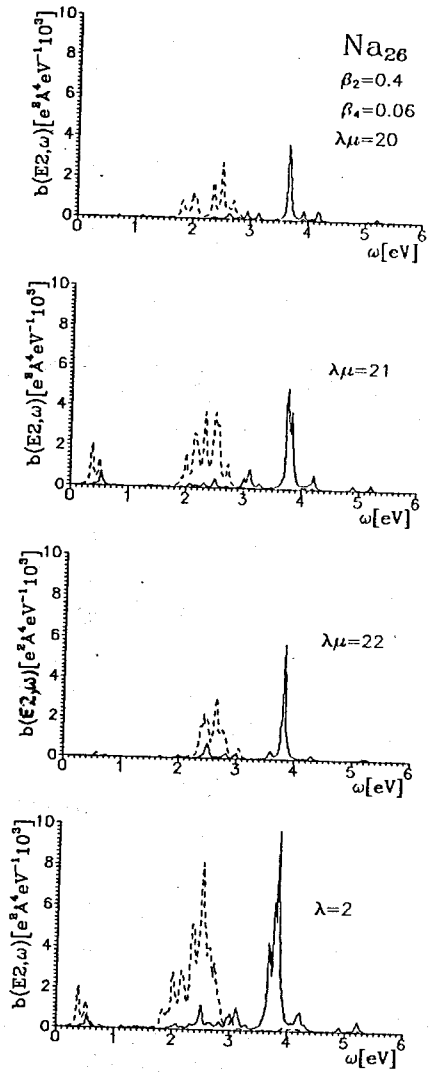

Fig.8 The strength function $b(E2,\omega) \equiv b_{m=0}(E2,\omega)$ for E2 excitations in Na_{26}. The plots are given for each projection $\mu = 0,1,2$ and for the total case (in the bottom). In every plot the results obtained with (solid line) and without (dashed line) residual interaction are presented.

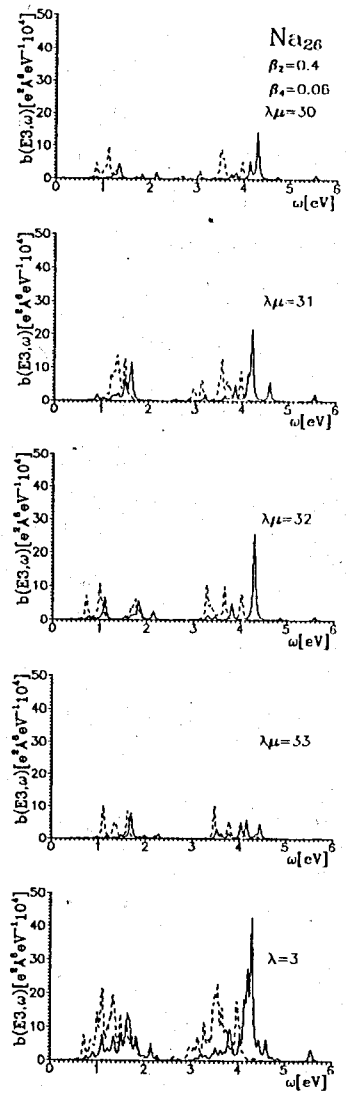

Fig.9 The strength function $b(E3,\omega) \equiv b_{m=0}(E3,\omega)$ for E3 excitations in Na_{26}. The plots are given for each projection $\mu = 0,1,2,3$ and for the total case (in the bottom). In every plot the results obtained with (solid line) and without (dashed line) the residual interaction are presented.

Acknowledgments

We are grateful to Profs. M.Brack, E.Lipparini and P.-G.Reinhard, Drs. Th.Hirschmann and M.Rotter for useful discussions. We are obliged to Drs. Th.Hirschmann and M.Rotter for letting of the deformation parameters for Na_{10}. One of the authors (V.O.N.) is grateful for financial support from Russian Science Foundation (grant 94-02-04615).

Appendix

After the multipole expansion of the single-particle potential and density the inverse strength constant (11) can be written as:

$$\kappa^{-1}_{\lambda\mu d} = -\sum_{lm}\sum_{l'm'}\sum_{LM}(-1)^M C^{LM}_{lm\lambda\mu}(C^{L-M}_{lm\lambda\mu} + d(-1)^\mu C^{L-M}_{lm\lambda-\mu}) \cdot (L^{lml'm'(v)}_{\lambda L} + L^{lml'm'(c)}_{\lambda L})$$

where

$$L^{lml'm'(v)}_{\lambda L} = \frac{\lambda(2\lambda-1)(2\lambda+1)^2}{2\pi(2L+1)}\int_0^\infty dr r^{2\lambda-2}$$

$$\cdot[L^{(1)}_{\lambda Lll'}dn_{l'm'}/dr \cdot dV_{lm}/dr \cdot r^2 + L^{(2)}_{\lambda Lll'}n_{l'm'} \cdot dV_{lm}/dr \cdot r + L^{(3)}_{\lambda Lll'}n_{l'm'} \cdot V_{lm}],$$

$$L^{lml'm'(c)}_{\lambda L} = \frac{8\lambda(2\lambda-1)(2\lambda+1)^2}{(2L+1)^2}\int_0^\infty dr r^\lambda$$

$$\cdot[L^{(4)}_{\lambda Lll'}n_{l'm'}(r) \cdot n_{lm}(r) \cdot r^\lambda + L^{(5)}_{\lambda Lll'}n_{l'm'}(r) \cdot r^{-(L+1)}\int_0^r n_{lm}(r_1) \cdot r_1^{\lambda+L}dr_1$$

$$+L^{(6)}_{\lambda Lll'}n_{l'm'}(r) \cdot r^L \int_r^\infty n_{lm}(r_1) \cdot r_1^{\lambda-L-1}dr_1].$$

The coefficients used in these expressions and in expressions (14)-(15) have the following form:

$$M^{(1)}_{\lambda Ll} = A_{\lambda Ll} - B_{\lambda Ll},$$

$$M^{(2)}_{\lambda Ll} = l \cdot A_{\lambda Ll} + (l+1) \cdot B_{\lambda Ll},$$

$$M^{(3)}_{\lambda Ll} = (l+\lambda+L+1) \cdot A_{\lambda Ll} + (l-\lambda-L)) \cdot B_{\lambda Ll},$$

$$M^{(4)}_{\lambda Ll} = (l+\lambda-L) \cdot A_{\lambda Ll} + (l-\lambda+L+1)) \cdot B_{\lambda Ll}$$

where

$$A_{\lambda Ll} = \sqrt{(l+1)(2l+3)}\begin{pmatrix} l+1 & \lambda-1 & L \\ \lambda & l & 1 \end{pmatrix} \cdot C^{L0}_{l+10\lambda-10},$$

$$B_{\lambda Ll} = \sqrt{l(2l-1)}\begin{pmatrix} l-1 & \lambda-1 & L \\ \lambda & l & 1 \end{pmatrix} \cdot C^{L0}_{l-10\lambda-10}.$$

Further,

$$L^{(1)}_{\lambda Lll'} = M^{(1)}_{\lambda Ll'} \cdot M^{(1)}_{\lambda Ll},$$

$$L^{(2)}_{\lambda Lll'} = M^{(1)}_{\lambda Ll'} \cdot M^{(2)}_{\lambda Ll} - M^{(2)}_{\lambda Ll'} \cdot M^{(1)}_{\lambda Ll},$$

$$L^{(3)}_{\lambda Lll'} = ((2\lambda-1)M^{(1)}_{\lambda Ll'} + M^{(2)}_{\lambda Ll'}) \cdot M^{(2)}_{\lambda Ll},$$

$$L^{(4)}_{\lambda Lll'} = M^{(1)}_{\lambda Ll'} \cdot \cdot (M^{(3)}_{\lambda Ll} - M^{(4)}_{\lambda Ll}).$$

$$L^{(5)}_{\lambda Lll'} = ((\lambda-L)M^{(1)}_{\lambda Ll'} - M^{(2)}_{\lambda Ll'}) \cdot M^{(3)}_{\lambda Ll},$$

$$L^{(6)}_{\lambda Lll'} = ((\lambda+L+1)M^{(1)}_{\lambda Ll'} + M^{(2)}_{\lambda Ll'}) \cdot M^{(4)}_{\lambda Ll},$$

For spherical systems we have $l = m = 0$, $L = \lambda$ and

$$B_{\lambda\lambda 0} = M^{(2)}_{\lambda\lambda 0} = M^{(4)}_{\lambda\lambda 0}$$

$$= L^{(2)}_{\lambda\lambda 00} = L^{(3)}_{\lambda\lambda 00} = L^{(5)}_{\lambda\lambda 00} = L^{(6)}_{\lambda\lambda 00} = 0,$$

$$M^{(1)}_{\lambda\lambda 0} = A_{\lambda\lambda 0} = \sqrt{\frac{\lambda}{(2\lambda-1)(2\lambda+1)}},$$

$$M^{(3)}_{\lambda\lambda 0} = A_{\lambda\lambda 0}(2\lambda+1) = \sqrt{\frac{\lambda(2\lambda+1)}{(2\lambda-1)}},$$

$$L^{(1)}_{\lambda\lambda 00} = A^2_{\lambda\lambda 0} = \frac{\lambda}{(2\lambda-1)(2\lambda+1)},$$

$$L^{(4)}_{\lambda\lambda 00} = A^2_{\lambda\lambda 0}(2\lambda+1) = \frac{\lambda}{(2\lambda-1)}.$$

REFERENCES

1. de Heer, W.A. et al: Phys.Rev.Lett. **59** 1805 (1987)
2. vom Felde, A., Fink, J. and Ekardt, W.: Phys.Rev.Lett. **61**, 2249 (1988)
3. Brechignac, C. et al: Chem.Phys.Lett. **164** 433 (1989)
4. Fallgren, H. and Martin, T.P.: Chem.Phys.Lett. **168** 233 (1990)
5. Selby, K. et al.: Phys.Rev. B**40**, 5417 (1989)
6. Selby, K. et al.: Z.Phys.D **19**, 43 (1991)
7. Borgreen, J. et al: Phys.Rev. B**48**, 17507 (1993)
8. de Heer, W.A.: Rev.Mod.Phys. **65**, 611 (1993)
9. Brack, M.: Rev.Mod.Phys. **65**, 677 (1993)
10. Hirschmann, Th., Brack, M. and Mejer, J.: Annalen Physik **3**, 336 (1994)
11. Reinhard, P.-G., Brack, M. and Genzken, O.: Phys.Rev. A**41**, 5568 (1990)
12. Montag, B., Reinhard, P.-G. and Mejer, J.: to be published in Z.Phys.D. (1994)
13. Kresin, V.V.: Phys.Rep. **220**, 1 (1992)
14. Pacheco, J.M. and Ekardt, W.: Z.Phys. D**24**, 65 (1992)
15. Lipparini, E. and Stringari, S.: Z.Phys. D**18**, 193 (1991)
16. Iachelo, F., Lipparini, E. and Ventura, A.: Phys.Rev. B**45**, 4431 (1992)
17. Yannouleas, C., Vigezzi, E. and Broglia, R.A.: Phys.Rev. B**47**, 9849 (1993)

18. Broglia, R.A. et al: Z.Phys.D **31**, 181 (1994)
19. Serra, Ll. et al.: Phys.Rev. **B39**, 8247 (1989)
20. Serra, Ll., Garcias, F., Barranko, M. et al: Phys.Rev. B**41**, 3434 (1990)
21. da Providencia, J. and de Haro, Jr.R.: Phys.Rev. B**49**, 2086 (1994)
22. Nesterenko, V.O.: Sov.J.Part.Nucl. **23**, 1665 (1992)
23. Brack, M.: Phys.Rev. B**39**, 3533 (1989)
24. Ekardt, W.: Phys.Rev. B**29**, 1558 (1984)
25. De Heer, W.A., Knight, W.D., Chou, M.Y. and Coneh, M.L.: Solid State Phys. **40**, 93 (1987)
26. Kohn, W. and Sham, L.J.: Phys.Rev. 1965, **140**, 1133A (1965)
27. Lang, N.D. and Kohn, W.: Phys.Rev. B**1**, 4555 (1970)
28. Clemenger, K.: Phys.Rev. B**32**, 1359 (1985)
29. Nishioka, H., Hansen, Kl. and Mottelson, B.R.: Phys.Rev. B**42**, 9377 (1990)
30. Lauritsch, G., Reinhard, P.-G. and Brack, M.: Phys.Lett. A**160**, 179 (1990)
31. Reimann, S.M., Brack, M. and Hansen, K.: Z.Phys.D **28**, 235 (1991)
32. Hirschmann, Th., Brack, M. and Mejer, J.: Ann.Phys. **3**, 336 (1994)
33. Frauendorf, S. and Pashkevich, V.V.: Z. Phys. D**26**, S-98 (1993)
34. Frauendorf, S. and Pashkevich, V.V.: Preprint FZR-37, Rossendorf, 1994, submit. to Phys.Rev.B.
35. Yannouleas, C. and Landman, U.: to be published in Phys.Rev. B**15**

36. Rowe, D.J.:In: Nuclear Collective Motion, Methuen, London, 1970

37. Bohr, A. and Mottelson, B.R.:In: Nuclear Structure, v.2, Benjamin, New-York, 1975

38. Hamamoto, I.: Physica Scripta **6**, 266 (1972)

39. Suzuki, T. and Rowe, D.J.: Nucl.Phys. **A289**, 461 (1977)

40. Lipparini, E. and Stringari, S.: Nucl.Phys. **A371**, 430 (1981)

41. Nazmitdinov, R. and Aberg, S.: Phys.Lett. **289B**, 238 (1992)

42. Nesterenko, V.O., Preprint JINR E4-93-338, Dubna (1993)

43. Nesterenko, V.O., Kleinig, W. and Shirikova, N.Yu.: Izv.Akad.Nauk, ser.fiz., **58**, 16 (1994)

44. Nesterenko, V.O. and Kleinig, W.: to be published in Phys.Scr.

45. Malov, L.A., Nesterenko, V.O. and Soloviev, V.G.: Teor.Mat.Fiz. **32**, 134 (1977)

46. Stringary, S.: Ann.Phys. **151**, 35 (1983)

47. Arvati, S., Dona dalle Rose, L.F., Silvestrelli, P.L. and Toigo, F.: Nuovo Cim. **11D**, 1063 (1989)

48. Hirschmann, Th. and Rotter, M.: to be published.

Received by Publishing Department
on December 28, 1994.

Нестеренко В.О., Клейниг В., Гудков В.В. E4-94-510

Коллективные $E\lambda$-возбуждения поверхностного типа в сферических и деформированных натриевых кластерах: модель вибрирующего потенциала

Обобщена самосогласованная модель вибрирующего потенциала (МВП) для описания $E\lambda$-возбуждений поверхностного типа в металлических кластерах с практически произвольной статической деформацией (включая сферический случай). В расчетах могут быть использованы любые одночастичные потенциалы и плотности валентных электронов, для которых известны коэффициенты мультипольного разложения. Использованный в модели метод силовой функции позволяет избежать решения уравнений для каждого состояния и тем самым кардинально упрощает вычисления. Модель имеет достаточно общий характер и, если пренебречь кулоновскими членами, может применяться для описания гигантских изоскалярных резонансов в атомных ядрах. Рассматриваются результаты расчетов в рамках МВП для E1-, E2-и E3-возбуждений в сферических (Na_8, Na_{20} и Na_{40}) и деформированных (Na_{10}, Na_{18} и Na_{26}) кластерах.

Работа выполнена в Лаборатории теоретической физики им. Н.Н.Боголюбова ОИЯИ.

Препринт Объединенного института ядерных исследований. Дубна, 1994

Nesterenko V.O., Kleinig W., Gudkov V.V. E4-94-510

Collective $E\lambda$-Excitations of Surface Character in Spherical and Deformed Sodium Clusters: Vibrating Potential Model

The self-consistent vibrating potential model (VPM) is extended for the description of $E\lambda$ surface collective excitations in alkali metal clusters with practically any kind of static deformation. The case of spherical clusters is also covered. Any single-particle potentials and valence electron densities for which the coefficients of the multipole expansion are known can be used within the model. The strength function method incorporated into the model allows one to avoid solving the equations for every state and, as a result, simplifies the calculations drastically. The model is of a quite general character and can also be used for description of isoscalar giant resonances in atomic nuclei if the Coulomb terms are neglected. The VPM is applied to calculate the E1, E2 and E3 excitations in spherical (Na_8, Na_{20} and Na_{40}) and deformed (Na_{10}, Na_{18} and Na_{26}) clusters.

The investigation has been performed at the Bogoliubov Laboratory of Theoretical Physics, JINR.

Preprint of the Joint Institute for Nuclear Research. Dubna, 1994